American Mineralogist
Vol. 57, pp. 1232–1241 (1972)

STABILITY OF IRON-FREE PIGEONITE AT ATMOSPHERIC PRESSURE

HOUNG-YI YANG[1] AND W. R. FOSTER, *Department of Mineralogy, The Ohio State University, Columbus, Ohio 43210*

ABSTRACT

Iron-free pigeonite, a phase distinct from clinoenstatite solid solution, is shown to be stable at atmospheric pressure. A primary field of crystallization for iron-free pigeonite is delineated in the system forsterite–diopside–silica.

The stability of iron-free pigeonite is evident from the morphology and compositions of crystals synthesized close to the liquidus temperatures from glasses with compositions in the field previously labeled protoenstatite. Crystals with monoclinic morphology crystallize below 1432°C and with orthorhombic morphology above 1432°C. Microprobe analysis of the crystals indicates a compositional gap in CaO content between the monoclinic and orthorhombic crystals. The discontinuity of the solidus curve in the Mg-rich region of the system $MgSiO_3$–$CaMgSi_2O_6$ is clearly shown.

Terrestrial pigeonites containing less than 20 mole percent $FeSiO_3$ have not been reported. From consideration of the composition and the temperature of stability limit, such low-iron pigeonites may occur in the chondrules of the least recrystallized chondrites, such as Type II and III carbonaceous chondrites and the "unequilibrated" ordinary chondrites.

INTRODUCTION

The system $MgSiO_3$–$CaMgSi_2O_6$ has been repeatedly investigated for many decades, yet there are still some uncertainties regarding the phase relations in the Mg-rich portion of the system where the phase equilibrium studies have been complicated by non-quenchable inversions. Boyd and Schairer (1964) pointed out the existence of an unrecognized Mg-rich pyroxene above 1365°C. Perrotta and Stephenson (1965) observed directly at high temperatures a reversible inversion in clinoenstatite of supposed composition $(Mg_{0.925}Ca_{0.075})SiO_3$, and indexed the X-ray powder pattern on a triclinic cell. Smith (1969a, b) reindexed the pattern as a mixture of olivine, silica mineral, and a dominant pyroxene with much larger c and V than clinoenstatite. He suggested that the space group was $C2/c$ and that increasing vibration of Mg(2) caused the silicate chains to straighten out. Kushiro (1968) and Kushiro and Yoder (1969) successfully synthesized iron-free pigeonite with a composition near $(Mg_{0.9}Ca_{0.1})SiO_3$ between 1450°C and 1600°C at a pressure between 5kb and 20kb. All of these results point to the possible occurrence of a stability field near $(Mg_{0.9}Ca_{0.1})SiO_3$ in the system $MgSiO_3$–$CaMgSi_2O_6$ and a primary field of crystallization in the system

[1] Present address: Code 644, Goddard Space Flight Center, NASA, Greenbelt, Maryland 20771.

forsterite–diopside–silica for a monoclinic magnesian pyroxene at atmospheric pressure above 1365°C.

The authors investigated this possibility by studying the morphology, compositions, optical properties, and structures of the euhedral crystals crystallized just below the liquidus temperatures from glasses with compositions in the field previously labeled protoenstatite.

Experimental Methods

Conventional quenching methods developed at the Geophysical Laboratory (Schairer, 1959) were used to synthesize the euhedral crystals of magnesian pyroxenes. Homogeneous glasses were prepared by repeated fusions of appropriate proportions of purified raw materials: calcium carbonate, magnesium carbonate, and silica. A small amount of devitrified glass was wrapped in a platinum envelope and hung in the hot zone of a quenching furnace long enough for the attainment of equilibrium, followed by quenching in mercury to preserve the crystals formed at high temperatures. Criteria discussed by Schairer (1959) were used to establish the attainment of equilibrium. The temperatures were read from a Pt–Pt10 percent Rh thermocouple calibrated periodically against the melting point of diopside (1391.5°C).

The morphology and optical properties of the quenched crystals were studied by petrographic microscopy, and the structures were examined by X-ray powder diffraction. Polished epoxy mounts of powdered quenching charges were prepared, and crystals larger than 25 micrometers were analyzed with an electron microprobe. An ARL-EMX microprobe was operated at 15 KV with a beam current of 0.15 μA and a beam diameter of about two micrometers. A synthetic diopsidic glass was used as the standard. Corrections, following the procedures of Sweatman and Long (1969), were made for deadtime, drift, background, fluorescence, absorption, and atomic number effects.

Magnesian Pyroxenes

Morphology. Well-developed, euhedral crystals of magnesian pyroxenes were obtained when devitrified glasses were held at temperatures just below the liquidus. The crystals range from a few to fifty micrometers in size and very often show clear crystal edges and faces. Thus, crystals with monoclinic morphology could be distinguished easily from those with orthorhombic morphology under the microscope. The crystal forms of magnesian pyroxenes observed in the quenching runs are given in Table 1, together with the compositions of starting devitrified glasses and the equilibrium temperatures. Note that monoclinic crystals of magnesian pyroxene crystallized below 1432°C and orthorhombic crystals above 1432°C from the melts in the primary field previously believed to belong to protoenstatite.

The interfacial angles on the orthorhombic and monoclinic crystals measured with a universal stage are given in Table 2. The crystal faces were plotted on gnomonic projections from which the crystals were

Table 1

Crystal Habit and Composition of Synthetic Magnesian Pyroxenes in the System Forsterite-Diopside-Silica

Glass Composition (wt.%)			Temperature	Time	Magnesian Pyroxene				
					Crystal	Composition (wt.%)			
Fo	Di	SiO_2	°C	Hrs.	Habit	CaO	MgO	SiO_2	Total
41.1	34.7	24.2	1463	1	Orthorhombic	-	-	-	-
			1470	1	Orthorhombic	0.54	40.87	58.25	99.66
33.8	46.4	19.8	1442	1	Orthorhombic	1.17	40.31	58.47	99.95
			1440	1	Orthorhombic	-	-	-	-
			1435	1	Orthorhombic	1.35	39.90	58.95	100.20
26.6	57.9	15.5	1420	2½	Monoclinic	2.59	38.65	59.12	100.36
			1411	6	Monoclinic	3.14	38.30	59.00	100.44
			1409	2	Monoclinic	-	-	-	-
17.6	63.6	18.8	1397	1	Monoclinic	3.72	38.02	58.28	100.02
			1394	2	Monoclinic	3.86	37.44	58.46	99.76
			1390	1½	Monoclinic	-	-	-	-
21.6	55.7	22.7	1415	1	Monoclinic	-	-	-	-
			1403	1½	Monoclinic	-	-	-	-
			1388	24	Monoclinic	-	-	-	-
			1387	84	Monoclinic	4.92	36.80	58.66	100.38
			1380	48	Monoclinic	-	-	-	-
			1376	96	Monoclinic	-	-	-	-
26.1	54.1	19.8	1429	¾	Monoclinic	-	-	-	-
			1423	2½	Monoclinic	-	-	-	-
			1418	2	Monoclinic	-	-	-	-

drawn (Figure 1). Angle tables were calculated for both habits of the crystals (Tables 3 and 4). All of the forms on the monoclinic crystals are prominent except {001} which is less conspicuous. Concave terminal faces resulting from twinning are not uncommon.

There are similarities in morphology between the orthorhombic crystals and the inverted clinoenstatite described from Papua by

Table 2

Interfacial Angles Measured on Synthetic Magnesian Pyroxenes

Orthorhombic Crystal		Monoclinic Crystal	
(010) ∧ (110)	50°	(010) ∧ ($\bar{3}$31)	52°
(110) ∧ (1$\bar{1}$0)	80°	(010) ∧ ($\bar{1}$11)	73°
(100) ∧ (110)	40°	(010) ∧ (021)	60°
(100) ∧ (111)	57°	(010) ∧ (110)	49°
(110) ∧ (111)	44°	(010) ∧ (100)	90°
(100) ∧ (234)	71°	(100) ∧ (101)	60°
(010) ∧ (234)	66°	(100) ∧ (001)	76°
(010) ∧ (100)	90°	(010) ∧ (001)	90°
		(010) ∧ (101)	90°

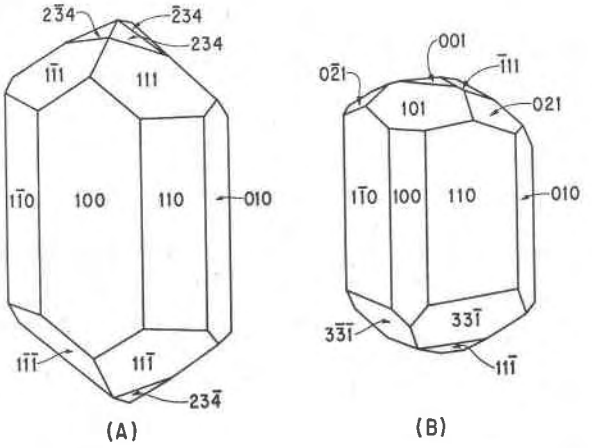

FIG. 1. The primary crystals of magnesian pyroxene: orthorhombic (A) and monoclinic (B), drawn in clinographic projection.

Dallwitz *et al.* (1966). For example, the angles (110) $\wedge$ ($\bar{1}$10) and (1$\bar{1}$0) $\wedge$ (110) on the inverted clinoenstatite are comparable to the equivalent interfacial angles on the synthetic orthorhombic crystals. In addition, Dallwitz *et al.* reported two bipyramids on the inverted clinoenstatite, consistent with two bipyramids on the synthetic orthorhombic crystals seen in Figure 1.

Optical Properties. The optical properties of both magnesian pyroxenes are given in Table 5. Though simple twinning is common in monoclinic magnesian pyroxene, polysynthetic twinning has not been found. In contrast, orthorhombic magnesian pyroxene frequently shows polysynthetic twinning optically, a phenomenon so often seen when protoenstatite inverts to clinoenstatite on quenching. Another noteworthy feature is that the small optic axial angle and the small $Z \wedge c$ of the monoclinic magnesian pyroxene are characteristic of natural pigeonites.

Symmetry. The symmetry of monoclinic magnesian pyroxene from the quenching run of 1387°C was studied by X-ray powder diffraction (Table 6). The appearance of the reflection (231) indicates that the symmetry of the monoclinic magnesian pyroxene is $P2_1/c$ at room temperature. Studies on the symmetry of the orthorhombic magnesian pyroxene are currently underway.

Composition. Accurate compositions of the monoclinic and orthorhombic magnesian pyroxenes from some quenching runs were obtained from microprobe analysis, and are given in Table 1. The CaO content in orthorhombic crystals increases from 0.54 $\pm$ 0.01 wt percent at 1470°C to 1.35 $\pm$ 0.02 wt percent at 1435°C, while it varies from 2.59 $\pm$ 0.03 wt

Table 3

Morphology of Monoclinic Crystals of the Synthetic Magnesian Pyroxenes

Crystal System = Monoclinic Crystal Class = $\frac{2}{m}$

$a:b:c = 0.905:1:0.313$ $\beta = 103°14'$ $p_o:q_o:r_o = 0.336:0.304:1$

$\mu = 76°46'$ $p'_o = 0.345$ $q'_o = 0.312$ $x_b = 0.235$

Forms	ϕ	ρ	ϕ_2	ρ_2 = B	C	A
001	90°	13°14'	76°46'	90°	0°	76°46'
010	0°	90°	90°	0°	90°	90°
100	90°	90°	0°	90°	76°46'	0°
101	90°	30°07'	59°53'	90°	16°53'	59°53'
021	21°	33°16'	76°46'	59°09'	30°51'	78°40'
110	49°	90°	0°	49°	80°02'	41°
$\bar{1}10$	-49°	90°	0°	-49°	99°57'	139°
$\bar{1}11$	-18°	17°56'	-84°17'	-72°58'	25°16'	95°28'
$\bar{3}31$	-39°30'	50°27'	-52°24'	-53°28'	59°28'	119°22'

percent at 1420°C in monoclinic crystals to 4.92 ± 0.05 wt percent at 1387°C. The existence of a compositional gap in CaO content between these two magnesian pyroxenes appears to be clear.

Discussion

The fact that, though crystals may invert during the quenching, their shapes can be preserved suggests a primary field of crystallization for the monoclinic magnesian pyroxene in the field previously labeled protoenstatite, as delineated in Figure 2. From further consideration of its characteristic optical properties and CaO content, it is evident that this monoclinic magnesian pyroxene is iron–free pigeonite, a phase

Table 4

Morphology of Orthorhombic Crystal of the Synthetic Magnesian Pyroxene

Crystal System = Orthorhombic Class = $\frac{2}{m}\frac{2}{m}\frac{2}{m}$

$a:b:c = 1.266:1.493:1$ $p_o:q_o:r_o = 0.79:0.67:1$

Form	ϕ	ρ=C	ϕ_1	ρ_1 = A	ϕ_2	ρ_2 = B
100	90°	90°	0°	0°	0°	90°
010	0°	90°	90°	90°	90°	0°
110	50°	90°	90°	40°	0°	50°
111	50°	46°	34°	56°35'	51°41'	62°30'
234	38°30'	32°37'	27°42'	70°23'	68°27'	65°02'

Table 5

Optical Properties of Monoclinic and Orthorhombic Magnesian Pyroxenes

Optical Properties	Monoclinic Magnesian Pyroxene	Orthorhombic Magnesian Pyroxene
Crystal habit	Short prismatic	Tabular on (100) Prismatic
Twinning	Simple twinning on (100)	None
Extinction	Oblique, $Z \wedge c = 25^{\circ}$	Parallel
Optical orientation	Y = b O.A.P. // (010)	Y = a X = b Z = c O.A.P. // (100)
Optic axial angle (measured)	$2V_Z = 26^{\circ}$	$2V_Z = 48^{\circ}$
Refractive indices (Na light)	$\alpha = 1.648(1)$	$\alpha = 1.648(1)$
	$\beta = 1.649(1)$	$\beta = 1.650(1)$
	$\gamma = 1.663(1)$	$\gamma = 1.658(1)$

Table 6

X-ray Diffraction Data of Monoclinic Magnesian Pyroxene, $(Mg_{0.91}Ca_{0.09})SiO_3$ *

a = 9.628(2) b = 8.856(2) c = 5.2048(2) $\beta = 108^{\circ}19'(7)$

I**	d(A) obs.	d(A) calc.	hkl	I**	d(A) obs.	d(A) calc.	hkl
5	3.297	3.298	021	<1	2.020	2.020	041
5	3.180	3.180	220	<1	1.940	1.942	$24\bar{1}$
10	2.987	2.987	221	1	1.792	1.791	510
8	2.887	2.890	$33\bar{1}$			1.772	222
		2.882	310	1	1.769	1.772	132
4	2.542	2.550	$13\bar{1}$			1.766	241
		2.531	$20\bar{2}$	<1	1.739	1.739	150
4	2.471	2.471	002	5	1.612	1.611	$53\bar{1}$
2	2.442	2.443	221	1	1.531	1.531	350
< 1	2.386	2.385	$23\bar{1}$	<1	1.493	1.494	$23\bar{3}$
2	2.215	2.214	040	1	1.484	1.484	$13\bar{3}$
< 1	2.148	2.150	112	1	1.476	1.476	060
4	2.124	2.123	$33\bar{1}$				
		2.120	330				

* Fe Kα/Mn; Camera diameter, 114.6 mm; Standard, NaCl

** Visual estimate

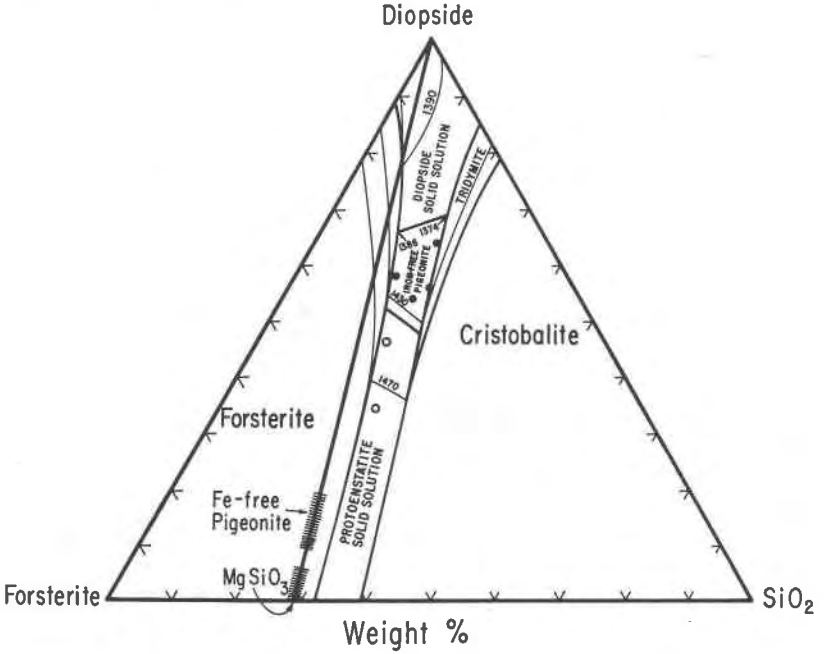

FIG. 2. The result of the present study as plotted on the system forsterite–diopside–silica of Kushiro and Schairer (1963). Solid circles: compositions from which monoclinic magnesian pyroxene crystallizes near liquidus. Open circles: compositions from which orthorhombic magnesian pyroxene crystallizes near liquidus.

distinct from inverted clinoenstatite solid solution. Boyd and Schairer (1964) reported that the (220) determinative curve for pyroxene in the single–phase field at 1395°C departs significantly from that for pyroxene at 1365°C, and made an important suggestion that there is an unrecognized form of Mg–rich pyroxene stable above 1385°C. Attention is called to the fact that the 2θ position of (220) of iron–free pigeonite with composition $(Mg_{0.91}Ca_{0.09})SiO_3$(28.06°, CuK$\alpha$ synthesized in the present study is very close to the determinative curve for pyroxene at 1395°C obtained by Boyd and Schairer. Perhaps the clinopyroxene with an anomalous cell size, obtained by Boyd and Schairer at 1395°C and thought to be an inversion product of an unrecognized form of Mg–rich pyroxene, is actually a primary phase and may well be identical to iron–free pigeonite synthesized in the present investigation. This relationship is further supported by the consideration of Smith (1969a, b) and Perrotta and Stephenson (1965) that a monoclinic form of magnesian pyroxene may be stabilized by a small substitution of Ca for Mg.

Consequently, when the data from microprobe analysis are incorporated, a stability field of iron-free pigeonite can be proposed in the system $MgSiO_3$–$MgCaSi_2O_6$ (Figure 3). While the upper stability limit of iron-free pigeonite is clearly at 1432°C, the lower limit has not been determined in this investigation, although there is likely to be one. Since Smyth (1970) has demonstrated a high-low inversion for an iron-rich clinopyroxene, confirming the consideration of Smith (1969a, b) that the space group of clinopyroxene may be $C2/c$ at high temperatures, iron-free pigeonite may also have undergone the same inversion during the quenching, which may not be recognized under the microscope. No high-temperature X-ray diffraction was undertaken in the present study, but $C2/c$ would be acceptable as the space group for iron-free pigeonite. Iron-free pigeonite shown to be stable at atmospheric pressure in this investigation may also be identical to the phase with composition $Mg_{1.9}Ca_{0.1}Si_2O_6$ and stable between 1360 ± 10°C and 1410 ± 10°C reported most recently by Schwab and Jablonski (1971).

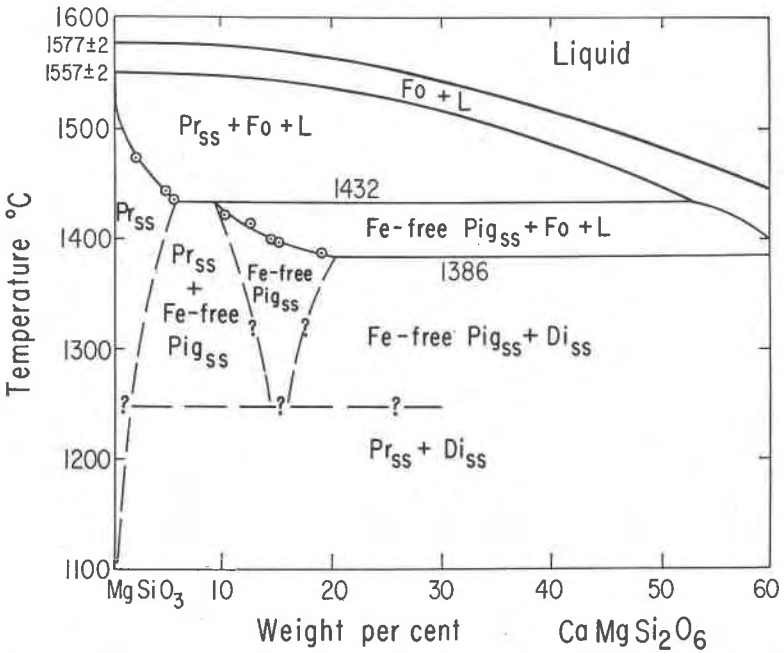

FIG. 3. Phase relation of Mg-rich portion of the system $MgSiO_3$–$CaMgSi_2O_6$ as suggested by the present investigation. Dotted circles: compositions of the primary crystals from microprobe analysis. Abbreviations: Fo, Forsterite; Pr_{ss}, Protoenstatite solid solution; L, Liquid; Di_{ss}, Diopside solid solution; Pig_{ss}, Pigeonite solid solution.

Geological Application

By substituting Fe^{2+} for Mg in iron-free pigeonite, the stability field of pigeonite is extended from the system $MgSiO_3$–$CaMgSi_2O_6$ into the pyroxene quadrilateral and the stability limit is gradually lowered as well. However, pigeonites with less than 20 mole percent $FeSiO_3$ have not been reported from terrestrial rocks. Present investigation suggests that iron–free pigeonite, or low–iron pigeonite, is stable only at a very reduced state and relatively high temperature. Such conditions are not common in the crystallization of terrestrial basaltic or andesitic rocks.

The occurrence of taenite and kamacite in chondrites and chondrules strongly suggests that most meteorites have been formed at a very reduced state. Although the origin of the chondrules is still disputable, some of the chondrules might have crystallized from the molten droplets at a temperature higher than the terrestrial volcanic rocks. Therefore, the chondrules in the relatively unrecrystallized chondrites, such as Type II and III carbonaceous chondrites and, in the sense of Dodd and Van Schmus (1965), "unequilibrated" chondrites, become the most likely places for low–iron pigeonites to occur.

The only indication of the occurrence of low–iron pigeonite was reported by Fredriksson and Reid (1965) in a chondrule from the Chainpur meteorite. This chondrule consists of olivine and clinopyroxene enclosed in a clear, homogeneous glass with a composition rich in albite component. The FeO and CaO contents of this clinopyroxene, analyzed with a microprobe, suggest that it is low–iron pigeonite.

Another conceivable mechanism for low–iron pigeonite to form is "shock melting" followed by rapid cooling in the meteorites. A temperature high enough for the crystallization of low–iron pigeonite may be reached locally. This possibility is supported by a report from Begemann and Wlotzka (1969) that the compositions of recrystallized clinopyroxene, from partial melting induced by shock, fall within the immicibility gap of the pyroxene quadrilateral. Fibrous clinopyroxenes embedded in devitrified glass are frequently encountered in the chondrules. They are customarily regarded as diopsidic clinopyroxenes despite the fact that some of them contain 3.0–3.4 percent of Ca (*e.g.*, in the Tennasilm meteorite, Reid and Fredriksson, 1967).

In conclusion, additional effort, particularly microprobe analysis, is needed to definitely establish the occurrence of low-iron pigeonite in the meteorites. Such studies are in progress.

Acknowledgment

This investigation was initiated in the Department of Mineralogy, The Ohio State University, where most of the quenching studies were made. Thanks are

due to Dr. Taki Negas for aid in the early stages of the work, and to the Edward Orton Jr. Ceramic Foundation, Columbus, Ohio, for fellowship support.

Research was completed in the Department of Geophysical Sciences, University of Chicago, where the microprobe work was done. The senior author is very grateful to Professor J. V. Smith for supervising the latter part of the study, for constructive comments on the manuscript, and for a postdoctoral appointment (NSF GA-21123).

References

Begemann, F., and F. Wlotzka (1969) Shock induced thermal metamorphism and mechanical deformations in Ramsdorf chondrite. *Geochim. Cosmochim. Acta,* **33**, 1351–1370.

Boyd, F. R., and J. F. Schairer (1964) The system $MgSiO_3$–$CaMgSi_2O_6$. *J. Petrology,* **5**, 275-309.

Dallwitz, W. B., D. H. Green, and J. E. Thompson (1966) Clinoenstatite in a volcanic rock from the Cape Vogel area, Papua. *J. Petrology,* **7**, 375–403.

Dodd, R. T., Jr., and W. R. Van Schmus (1965) Significance of unequilibrated ordinary chondrites. *J. Geophys. Res.* **70**, 3801–3811.

Fredriksson, K., and A. M. Reid (1965) A chondrule in the Chainpur meteorite. *Science,* **149**, 856–860.

Kushiro, I. (1968) Synthesis and stability of iron-free pigeonite in the system $MgSiO_3$–$CaMgSi_2O_6$ at high pressure. *Carnegie Inst. Wash. Year Book,* **67**, 80–83.

———, and J. F. Schairer (1963) New data on the diopside-forsterite-silica. *Carnegie Inst. Wash. Year Book,* **62**, 95–103.

———, and H. S. Yoder, Jr. (1969) Stability field of iron-free pigeonite in the system $MgSiO_3$–$CaMgSi_2O_6$. *Carnegie Inst. Wash. Year Book,* **68**, 226–231.

Perrotta, A. J., and D. A. Stephenson (1965) Clinoenstatite: High-low inversion. *Science,* **148**, 1090–1091.

Reid, A. M., and K. Fredriksson (1967) Chondrules and chondrites. *In* P. H. Abelson (ed.) *Research in Geochemistry,* **2**. John Wiley and Sons, New York, 170–203.

Schairer, J. F. (1959) Phase equilibria with particular reference to silicate systems. *In* J. O. Bockeris, J. D. Mackenzie, and J. L. White (eds.), *Physicochemical Measurements at High Temperatures.* Butterworths Scientific Publications, London, 117–134.

Schwab, R. G., and K. H. Jablonski (1971) Der Polymorphismus pigeonitischer Pyroxene. *Fortschr. Mineral.* **49**, (BH1), 48–50.

Smith, J. V. (1969a) Magnesium pyroxene at high temperature: Inversion in clinoenstatite. *Nature,* **222**, 256–257.

——— (1969b) Crystal structure and stability of the $MgSiO_3$ polymorph; physical properties and phase relations of Mg, Fe pyroxenes. *Mineral. Soc. Amer. Spec. Pap.* **2**, 3–29.

Smyth, J. R. (1970) *High Temperature Single-crystal Studies on Low-calcium Pyroxenes.* Ph. D. Thesis. University of Chicago, Chicago.

Sweatman, T. R., and J. V. P. Long (1969) Quantitative electronprobe microanalysis of rock-forming minerals. *J. Petrology,* **10**, 332–379.

Manuscript received, October 18, 1971; accepted for publication, February 10, 1972.